Precisely control mitochondrial membrane potential with light to manipulate cell fate decisions

Patrick Ernst[1], Ningning Xu[1], Jiajia Song[2], Jing Qu[2], Herbert Chen[3], Matthew S. Goldberg[4], Jianyi Jay Zhang[1], Brian O'Rourke[5], Xiaoguang Liu[1], and Lufang Zhou[1,2*]

Departments of Biomedical Engineering[1], Medicine [2], Surgery[3], and Neurology[4], University of Alabama at Birmingham, Birmingham, Alabama, USA, 35294

[5]Division of Cardiology, Department of Medicine, The Johns Hopkins University, Baltimore, Maryland, USA, 21205

Running title: Control Cell Fate Decisions with Light

* Correspondence:
Lufang Zhou, PhD
Division of Cardiovascular Disease
Department of Medicine
University of Alabama at Birmingham
703 19th Street South, ZRB 306
Birmingham, AL 35294, USA
Email: lfzhou@uab.edu
Phone: 205-975-3764

Keyword: parkin, cell death, mitochondria, autophagy, optogenetics

Abstract

Mitochondrial dysfunction has been implicated in aging, cardiovascular disease, cancer, neurodegeneration, and many other pathological conditions or diseases. The inner mitochondrial membrane (IMM) potential (*a.k.a.* $\Delta\Psi_m$) is essential for ATP synthesis *via* oxidative phosphorylation and also directly affects levels of reactive oxygen species, apoptosis, thermogenesis, and key signaling pathways. Better understanding the detailed mechanisms by which $\Delta\Psi_m$ regulates cellular function and fate decisions requires tools to manipulate $\Delta\Psi_m$ with spatial and temporal resolution, reversibility, or cell type specificity. To address this need, we have developed a new generation optogenetic-based technique for targeted mitochondrial depolarization with light. We demonstrate successful targeting of a heterologous Channelrhodopsin-2 (ChR2) fusion protein to the IMM and formation of functional cationic channels capable of light-induced targeted $\Delta\Psi_m$ depolarization, which was sufficient to cause translocation of the cytosolic protein Parkin to mitochondria and activation of mitochondrial autophagy. Importantly, we show that optogenetic-mediated mitochondrial depolarization can be well-controlled to differentially influence the fate of cells expressing mitochondrial ChR2: while mild, transient light illumination elicits cytoprotective effect, moderate, sustained light illumination induces apoptotic cell death. This new generation optogenetic tool may be useful for studying the effects of $\Delta\Psi_m$ depolarization on cell and organ function with spatial precision.

Introduction

Mitochondria lie at the crossroad of cellular metabolic and signaling pathways and thus play a pivotal role in regulating many intracellular processes such as energy production, reactive oxygen species (ROS) production, Ca^{2+} handling, and cell fate decision (1). Not surprisingly, defects of mitochondrial function have been implicated in a variety of human maladies such as aging, cardiovascular disease, cancer, and neurodegeneration (2). The normal functioning of mitochondria largely relies on maintaining the inner membrane potential ($\Delta\Psi_m$) to preserve the protonmotive force necessary to drive oxidative phosphorylation and redox balance. Interestingly, while profound depolarization of $\Delta\Psi_m$ is detrimental and induces cell injury (3), there is evidence that partial mitochondrial dissipation is cytoprotective (4,5). The detailed mechanism underlying the differential regulatory role of $\Delta\Psi_m$ on cell function and fate remains elusive, partially due to the difficulty of precisely controlling $\Delta\Psi_m$ or mitochondrial membrane permeability (MMP) in an experimental setting. Currently, manipulation of $\Delta\Psi_m$ is mainly *via* pharmacological intervention, i.e. using chemicals to uncouple the mitochondria (4,5) or to induce permeability transition pore (mPTP) opening (6). However, pharmacological approaches often cause unknown side effects and lack the ability to probe spatiotemporal domains. Several research groups, including us, use laser flashes to trigger local or cell wide mitochondrial depolarization *via* the photooxidation mechanism (7-9). A limitation of this approach is that it requires high-energy laser illumination, which may induce uncontrollable oxidative stress and unpredictable outcomes. A new approach capable of precisely controlling MMP or $\Delta\Psi_m$ is highly desired.

Optogenetics has recently emerged as a technique that utilizes genetically-encoded light-sensitive ion channels, such as channelrhodopsin 2 (ChR2) (10-13) or halorhodopsin (NpHR) (14,15), to precisely and remotely manipulate the activity of cells or animals (10,12). ChR2 is a seven-transmembrane domain protein that contains the light-isomerizable chromophore all-trans-retinal (16). When excited by blue light, the *all-trans* retinal undergoes *trans-cis* isomerization (17), activating non-selective cationic channels and inducing depolarizing inward currents. Due to its high spatiotemporal resolution, ChR2-based optogenetic techniques have evolved as a powerful tool in basic and translational research. For example, ChR2 has been expressed in neurons (18) to monitor and control their membrane potential, intracellular acidity, calcium influx, and other cellular processes (see ref (13) for a review). In addition, ChR2 has been used to manipulate the membrane excitability of cardiomyocytes (19-21), skeletal muscle cells (22) and cell lines expressing voltage-gated ion channels (23,24). Despite these advancements, there is few report

on the functional expression of ChR2 on the membrane of the mitochondrion, an organelle that requires fine control over ion transport for proper function, until very recently (25,26).

In addition to remote control of excitable cells, optogenetics techniques have been used to induce and study cell death. For instance, Yang *et al*. showed that an optogenetic approach can induce apoptotic cell death in human glioma cells *via* depolarization of cell membrane potential and influx of Ca^{2+} (27). In another study, Hill *et al.* reported a two-photon chemical apoptotic targeted ablation technique (28). By combining this technique with organelle-targeted fluorescent proteins and biosensors, they have successfully achieved precise ablation of specific populations of neurons in the mouse brain. Of note, none of the existing optogenetic approaches directly targets the inner mitochondrial membrane (IMM) permeability to induce cell death. We hypothesize that expression of ChR2 in the IMM of mammalian cells forms functional cationic channels capable of light-induced remote control of $\Delta\Psi_m$ depolarization and manipulation of cell fate decisions. We test this hypothesis using a variety of cell types and our results show that the mitochondrial leading sequence (MLS) of ABCB10, an ATP binding cassette transporter, can target ChR2 into IMM. We demonstrate that this new generation optogenetic approach can be used to induce controlled $\Delta\Psi_m$ depolarization and manipulation of cell fate decisions at high spatial resolution.

Results

Targeting ChR2 to the IMM. The MLS of cytochrome *c* oxidase subunit VIII (*a.k.a.* mito) has been widely used to import proteins such as GFP (29) or pericam (30) to mitochondria. Therefore, we first examined its capability to target ChR2 to mitochondria. A mutant of ChR2, ChR2(H134R) (31), was fused with eYFP and inserted into vector pCMV-myc-mito to generate plasmid mito-ChR2(H134R)-eYFP. The construct and the control vectors (mito-eYFP) were transfected to H9C2 cells, respectively. The expressions of ChR2-eYFP and eYFP in mitochondria were examined by staining mitochondria with Mitoracker® Deep Red and analyzing the colocalization of the green and red channels using confocal microscopy. Results show that eYFP was perfectly colocalized with mitochondria (Fig. S1A) but ChR2-eYFP was not (Fig. S1B). In addition, ChR2-eYFP appeared to be improperly processed by the endoplasmic reticulum (ER), implying that the size of the ChR2(H134R)-eYFP precursor might be impairing import. Thus, we next doubled the copy number of mito sequence and constructed plasmid $(mito)_2$-ChR2(H134R)-eYFP. However, this modification did not improve the import of ChR2(H134R)-eYFP to mitochondria (data not

shown). Thereafter, a series of mito-based ChR2-eYFP plasmids such as mito-ChR2 (H134R)-eYFP-ER (adding ER extraction sequence), mito-ChR2(H134R)(T2-23aa)-eYFP (removing the cell membrane targeting sequence) and $(mito)_3$-ChR2(H134R)-eYFP (to triplicate mito sequence) were constructed. Unfortunately, none of them could efficiently target ChR2-eYFP precursor to the mitochondria (data not shown). We also studied the MLS of ROMK, a candidate of mitochondrial K_{ATP} channel located on IMM (32). Similarly, ROMK MLS successfully imported eYFP into mitochondria (data not shown) but not ChR2-eYFP (Fig. S1C).

ATP binding cassette (ABC) transporters comprise a large family of membrane translocases (33) and are found in all species from microbe to human (34). Of them, ABCB10 is an IMM erythroid transporter with an unusually long MLS (140 amino acids) (35). Studies showed that ABCB10 MLS could lead various membrane proteins to mitochondria (36), while its depletion targeted ABCB10 to the ER (35). This MLS was fused with eYFP or ChR2(H134R)-eYFP, to generate ABCB-eYFP and ABCB-ChR2(H134R)-eYFP vectors, respectively, which were then transfected into H9C2 cells. To our great satisfaction, ABCB-eYFP was perfectly localized in mitochondria (Fig. 1A). Excitingly, ABCB10 MLS successfully translocated ChR2-eYFP precursor into H9C2 mitochondria, as demonstrated by the colocalization of green (eYFP) and red (MitoTracker) channels (Fig. 1B). Importantly, this method of targeting ChR2 to the IMM did not affect mitochondrial energetics, as demonstrated by the unaltered mitochondrial membrane potential and reactive oxygen species (ROS) level (Fig. S2). The disposition of ChR2-YFP fusion protein in H9C2 mitochondria was further examined by immunostaining. As shown in figure 1C, the ChR2 protein expression, detected by the ChR2 antibody, was colocalized with MitoTracker. The capability of ABCB10 MLS to translocate ChR2-eYFP to mitochondria was also confirmed in other cell types such as HeLa cells (Fig. 1D) and hiPSC-CMs (Fig. 1E). Altogether, our data demonstrate the localization of ChR2 within the mitochondria.

Light-elicited targeted mitochondrial depolarization. After demonstrating mitochondrial ChR2 expression, we examined if light could elicit targeted mitochondrial depolarization in ABCB-ChR2-expressing cells. In an experiment shown in figure 2, H9C2 cells expressing ABCB-ChR2 (fused with eYFP) were split into zone 1 and zone 2, with zone 1 receiving blue (475 nm) LED pulse illuminations and zone 2 receiving no illumination as control (Fig. 2A). The change of mitochondrial membrane potential was measured by TMRM using an Olympus confocal microscope (Fig. 2B). We found that the fluorescence of TMRM faded significantly in cells in zone 1 but not in zone 2 (Fig. 2C and Video S1). The averaged TMRM intensities before and after light illumination were summarized in figure 2D, which showed that $\Delta\Psi_m$ in zone 1 cells depolarized by

about 80% but in zone 2 cells remained unchanged. In addition to impaired mitochondrial membrane potential, light illumination also caused increased ROS production in ABCB-ChR2 expressing cells, as compared with control or ABCB-ChR2-expressing cells without blue light illumination (Fig S3). To verify that mitochondrial depolarization in zone 1 cells shown in figure 2 was caused by light-induced activation of ChR2 channels in IMM and not by imaging laser-induced photooxidation and photobleaching, we performed two control experiments. We first examined the effect of confocal imaging light alone on $\Delta\Psi_m$ in ABCB-ChR2-expressing cells. As shown in figure S4A (and Video S2A), in the absence of blue light illumination, confocal laser scanning had no effect on TMRM. However, concurrent application of blue light illumination led to significant $\Delta\Psi_m$ depolarization (Fig S4B and Video S2B) in a way similar to that observed in zone 1 cells shown in figure 2. In another experiment, we applied the same imaging conditions and illumination intensities as those used in the experiment shown in figure 2 to ABCB-eYFP-expressing cells. In the absence of ChR2 expression, neither eYFP nor TMRM fluorescent intensity changed after illumination (Fig. S5 and Video S3), indicating that light-elicited mitochondrial depolarization was not caused by mitochondrial eYFP expression. Together, these experiments demonstrate the functional expression of ChR2 on the IMM that allowed light-induced spatially-targeted mitochondrial depolarization.

Optogenetic-mediated light-induced Parkin mitochondrial translocation. To further confirm optogenetic-mediated mitochondrial depolarization, we examined whether blue light illumination elicits Parkin protein translocation to mitochondria, which is known to occur upon mitochondrial depolarization with ionophores such as CCCP (37). ABCB-ChR2-eYFP-expressing HeLa cells were transfected with mCherry-Parkin and subjected to LED illumination (24 hours, 0.5 mW/mm^2). The cellular localization of Parkin was examined by confocal microscopy at different time points during light treatment. As shown in figure 3A, at the baseline (i.e. 0 hour) mitochondria (represented by eYFP fluorescence) are tubular like and mCherry-Parkin was clearly cytosolic and diffuse, as expected. After 4 hours of LED illumination, mCherry-Parkin began to translocate from the cytosol to some mitochondria, as indicated by colocalization of Parkin and eYFP. After 8 hours of LED illumination, mitochondria became fragmented and mCherry-Parkin translocated to most of the mitochondria. After 24 hours, most of the mCherry-Parkin was found to surround mitochondria, as shown in the enlarged view of the boxed region, demonstrating that Parkin was recruited to mitochondrial outer membranes, similar to what occurs with CCCP-induced mitochondrial depolarization (37). On the contrary, no evident Parkin translocation to mitochondria was observed in either the un-illuminated ABCB-ChR2-eYFP-expressing cells (Fig 3B) or the light-illuminated ABCB-eYFP-expressing cells (Fig 3C) within 24

hours. Furthermore, light-illuminated ABCB-ChR2-eYFP-expressing HeLa cells displayed less mitochondrial mass compared with other groups, especially at 24 hours, suggesting induction of Parkin-dependent mitophagy. These data provide additional evidence of optogenetically-controlled mitochondrial depolarization in live cells.

Optogenetic-mediated light-induced cell death. Next, we examined the effect of sustained light illumination on ABCB-ChR2-expressing cells. Cell viability and cytotoxicity were measured using trypan blue staining, lactate dehydrogenase (LDH) assay, and alamarBlue assay, respectively. Continuous moderate LED illumination (0.5 mW/mm^2, 24 hours) had a negligible deleterious effect on the viability of control and mock-transfected HeLa cells (Fig S6), as well as ABCB-eYFP-expressing HeLa cells, but caused significant cell death in ABCB-ChR2-expressing HeLa cells (Fig. 4A). The LED illumination-induced cytotoxicity in ABCB-ChR2-expressing cells was confirmed by the LDH assay and alamarBlue assay. As shown in figure 4B, cell viability dropped nearly 80% in the light-illuminated ABCB-ChR2 cell cultures but only slightly in light-illuminated ABCB-eYFP-expressing HeLa cells. Consistent, substantial cytotoxicity was detected in light-illuminated ABCB-ChR2-expressing cells but not in the illuminated ABCB-eYFP-expressing cells (Fig 4C). Importantly, we found that pretreating cells with cyclosporine A, a selective mitochondrial permeability transition pore (mPTP) inhibitor, did not prevent the light-induced cell death (Fig 4D) and cytotoxicity (Fig 4E), indicating that the mitochondrial-targeted optogenetic-mediated cell death is independent of mPTP opening. This finding also denotes that ChR2 proteins formed ion channels in IMM that are functionally like mPTP to elicit cell death. Of note, antioxidants such as MitoTEMPO and MitoQ failed to rescue cells from light-induced cell death (data not shown), suggesting that ROS production is not a crucial factor in mitochondrial optogenetic-mediated cytotoxicity.

We then examined the time and light irradiance dependence of optogenetic-mediated cell death. As shown in figure 5A, viability of cell cultures dropped nearly linearly within 12 hours of light (0.5 mW/mm^2) illumination and tapered off slightly thereafter. Regarding the effect of light intensity, we found that six hours of moderate (e.g., 1 mW/mm^2 and 3 mW/mm^2) light illumination caused minimal cell death in ABCB-ChR2-expressing cell cultures, as measured by Hoechst and Propidium Iodide (PI) staining (Fig S7). Increasing light intensity to 5 mW/mm^2 or 7 mW/mm^2 caused a substantial (62% and 82%, respectively) decrease in cell viability (Fig 5B and 5C). Importantly, similar intensities (e.g., 3 mW/mm^2 and 5 mW/mm^2) of light illumination did not elicit detectable cell death in control cultures (Fig 5B, 5C and Fig S7).

Molecular mechanisms underlying optogenetic-mediated cell death. To explore the mechanistic pathways underlying the mitochondrial optogenetic-mediated cell death, we treated cells with an apoptosis inhibitor and necroptosis inhibitor, respectively. Cell death analysis showed that Z-VAD-FMK (20μM), a caspase inhibitor, substantially reduced light illumination-induced cell death, but 7-Cl-O-Nec-1 (100μM), a necroptosis inhibitor, had little effect on cell viability (Fig 6A), suggesting that the optogenetic-mediated light-induced cell death is likely through the caspase-dependent apoptotic pathway. We also noticed that mitochondrial membrane potentials were less depolarized in Z-VAD-FMK-treated cell cultures upon light illumination (Fig 6B). The light illumination-elicited activation of the intrinsic apoptosis pathway in ABCB-ChR2-expressing cells was confirmed by cytochrome C release experiments. As shown in figure 6C, immunocytochemistry revealed that cytochrome C was colocalized with TOM20, a mitochondrial outer membrane protein, in both the control cells and ABCB-ChR2-expressing cells not illuminated by LED light. However, light-illuminated ABCB-ChR2-expressing cells showed a punctate/diffuse cytochrome C staining, which was disparate from TOM20 immunostaining, indicating the release of cytochrome C into the cytosol (Fig 6C).

We next asked whether Parkin overexpression and activation of the canonical PINK1/Parkin-mediated mitophagy pathway reduces optogenetic-mediated cell death. ABCB-ChR2-expressing HeLa cells, with or without concurrent Parkin expression, were illuminated with light (24 hours, 0.5 mW/mm^2) and then subjected to $\Delta\Psi_m$ and cell death analysis. As expected, expression of Parkin did not affect mitochondrial membrane potential (Fig. 7A) and cell viability (data not shown) in the absence of light illumination. However, expression of Parkin surprisingly exacerbated light-induced mitochondrial depolarization (Fig 7A). In addition, although Parkin expression did not cause evident difference in cell viability in ABCB-ChR2-expressing cells immediately after 24 hours light illumination, significantly more severe cell death was detected in the Parkin-expressing HeLa cells 24 hours after stopping LED illumination (Fig 7B). The pro-apoptotic effect of Parkin activation has been reported in recent studies (38,39). Furthermore, in our hands Parkin did not abrogate or promote cell death in FCCP-treated (10 μM, 24 hours) HeLa cells (data not shown).

Mitochondrial optogenetic-mediated preconditioning and cytoprotection. Finally, we examined if mitochondrial optogenetic-mediated light-induced partial mitochondrial depolarization protects ABCB-ChR2-expressing cells against apoptotic cell death. As shown in figure 8, 6 hours moderate light (4 mW/mm^2) illumination caused 55% decrease in cell viability, which was consistent with data reported in figure 5. Intriguingly, cell viability in cultures pretreated with 2

hours mild (0.2 mW/mm^2) light illumination was significantly higher compared with the control group (i.e. without pretreatment).

Discussion

Application of the innovative optogenetic technique to manipulate intracellular organelles such as mitochondria has been limited. One challenge to developing a mitochondrial-based optogenetic approach is targeted expression of light-gated channel proteins in the highly folded IMM. In the present study, we have examined the capability of several commonly used MLS, including cytochrome C MLS (*a.k.a.* mito), to target the heterologous ChR2 proteins to mitochondria. While Taktch *et al.* have reported that tandem repeat mito sequence can target ChR2 to mitochondria (25), it causes poor mitochondrial localization of ChR2 in our hands. Instead, we provide evidence that the ABCB10 MLS can effectively translocate ChR2 to the IMM in a variety of cells types including H9C2, HeLa and cardiomyocyte cells. We further demonstrate that the expressed ChR2 proteins form functional cationic ion channels in the IMM, enabling targeted induction of mitochondrial depolarization by blue light. We confirm the optogenetic-mediated $\Delta\Psi_m$ dissipation by measuring $\Delta\Psi_m$ using confocal live cell imaging and flow cytometry assay, as well as by the translocation of Parkin from the cytosol to mitochondria, which is a well-established marker of mitochondrial depolarization.

The advantages of the optogenetic-based approach over the conventional pharmacological methods to induce mitochondrial depolarization include high spatial resolution *via* optics and specific targeting of ChR2 using cell type-specific promoters or vectors. The light stimulus can be controlled over the high spatial extent, particularly at subcellular dimensions, due to its optical nature. Thus, optogenetic-based light illumination would allow controllable manipulation of individual mitochondria or a group of mitochondria within a single cell. The capability of inducing mitochondrial membrane permeability in specific mitochondria with light can enable novel research, such as investigating how $\Delta\Psi_m$ impacts mitochondrial dynamics and network properties, Ca^{2+} handling, motility, mitophagy, or ROS-dependent signal propagation within or across cells. Spatial resolution is especially important for studies of neurons, which have much of their mitochondrial mass located in distal axons or dendrites. There has been considerable debate regarding how neurons handle damaged or dysfunctional mitochondria with some studies concluding that Parkin-mediated mitophagy only occurs near mature lysosomes in the cell body and that retrograde transport is required for degradation of distal mitochondria, while others concluding that Parkin-mediated mitophagy occurs in distal axons without retrograde transport to

the soma (40,41). Moreover, there may be distinct mechanisms by which neurons handle proximal vs. distal dysfunctional mitochondria and it is important to better define these mechanisms given that mitochondrial dysfunction is implicated in many neurodegenerative diseases and that degeneration of distal axon terminals may be one of the earliest stages and a better therapeutic target (42). The methods described here are ideally suited for investigating this because illumination can selectively depolarize only distal or only proximal mitochondria *in vitro* or *in vivo* using fiber optics.

In addition to high spatial resolution, the optogenetics approach provides specific targeting of tissues or cell types. Chemical uncoupling agents, such as the ionophores FCCP and CCCP, are widely used for the induction of mitochondrial depolarization. However, interpretation of the results can be confounded, especially in intact cells, because of their known off-target effects. For instance, It has been reported that both FCCP and CCCP inhibit the movement of mitochondria in neurites of chick sensory neurons in culture (43). Studies also showed that FCCP mediates conductance of several ions (e.g., H^+, Na^+ and Cl^-) in the plasma membrane (44), affecting membrane electrical characteristics (such as causing cell depolarization) (45),(46). On the contrary, the mitochondrial optogenetics approach shown here allows direct light-elicited $\Delta\Psi_m$ depolarization by targeted expression of ChR2 proteins in the IMM. Moreover, compared with the conventional photoactivation method that requires high energy laser flash, optogenetic-mediated $\Delta\Psi$m depolarization requires very low energy (mW/mm^2 level), as optogenetics is not simply photoexcitation of targeted cells; rather, it delivers gain of function of precise events. The low intensity light illumination would minimize side effects (such as photobleaching) on the illuminated cells or the proximal un-illuminated cells.

Apoptosis is a process of programmed cell death that occurs in multicellular organisms. While it is well established that mitochondria play key roles in activating programmed cell death, the underlying detailed mechanisms remain incompletely understood. For instance, the role of inner membrane permeabilization in the execution of pro-apoptotic protein (e.g. cytochrome C) release from the intermembrane space into cytosol is a subject of ongoing controversy. Some studies show that mitochondrial depolarization and IMM permeabilization are required for cytochrome C release and apoptotic cell death (47). However, others suggest that cytochrome C release can occur in the absence of $\Delta\Psi_m$ depolarization (48), mitochondrial depolarization may not be involved in the activation of apoptosis (49), or PTP opening is a consequence of apoptosis (47). The disparity may be attributed to the methods used in different studies, such as pharmacological intervention versus genetic manipulation. In the present study, using the mitochondrial

optogenetics approach we demonstrate that increased IMM permeability alone is sufficient to trigger apoptotic cell death, which is time and (light) dosage dependent. The activation of intrinsic apoptosis is confirmed by induction of cytochrome C release and prevention of cell death by a caspase inhibitor. Importantly, blocking mPTP did not prevent the light-induced cell death, which provides additional evidence that the expressed ChR2 formed functional cationic pores in IMM. Importantly, we show that mild short-term light illumination prevented apoptotic cell death in ABCB-ChR2-expressing cells, supporting the notion of mitochondrial preconditioning. Thus, this innovative mitochondrial optogenetics technique can be used to well control IMM depolarization and differentially influence cell fate, a capability not possessed by the existing pharmacological approaches.

Loss-of-function mutations in Parkin have been causally linked to early-onset Parkinson's disease (50). In addition, studies have shown that Parkin overexpression can prevent cell death in response to a variety of stimuli (51-53). Thus, considerable enthusiasm has emerged recently regarding the potential of Parkin as a therapeutic target. However, here we surprisingly observe that activation of Parkin exacerbates light-induced mitochondrial depolarization and cell death. While our findings appear contradictory to the conventional notion that Parkin is cytoprotective, the pro-apoptotic effect of Parkin has been reported in two recent studies (38,39). The apparent paradoxical role of Parkin appears attributed to the nature of the stressor to induce cell death, i.e., whether the stimulus induces mitochondrial depolarization and activation of Parkin. For instance, Carroll *et al.* (38) have shown that Parkin overexpression enhances HeLa cell apoptosis induced by mitochondrial depolarizing agents such as CCCP and valinomycin but has no effects on cell death induced by other stimuli that fail to activate Parkin. Similarly, Zhang *et al.* reported that Parkin activation significantly exacerbates valinomycin-induced apoptosis but does not promote CCCP-induced cell death in HeLa cells (39). They further demonstrated that the level of Parkin recruitment-induced Mcl-1 degradation and polyubiquitination is a key factor determining whether Parkin-dependent mitophagy versus apoptotic cell death is activated. While the reason underlying the discriminate effect of Parkin on the fate of CCCP-treated cells in those two studies requires further investigation, the severity of mitochondrial damage might be a critical factor. If mitochondrial damage is too severe to be repaired by mitophagy, the PINK1/Parkin pathway may promote apoptosis. The effect of Parkin on cell death decisions may also depend the level of its activation: with transient activation inducing mitophagy to repair mitochondrial networks and sustained activation triggering apoptosis to eliminate damaged cells. Our findings warrant consideration when designing Parkin-based therapeutic strategies.

One limitation of the developed mitochondrial optogenetics technique is that although it enables targeted mitochondrial depolarization at high spatial (cellular or subcellular) resolution, the time resolution of light-induced mitochondrial depolarization is much less. Similar to that shown in a recent study (25), optogenetic-induced mitochondrial depolarization takes several minutes to accomplish. Using other rhodopsin protein variants with higher conductance or greater light sensitivity may help to achieve better temporal control of mitochondrial depolarization (54). The lack of mitochondrial repolarization may be partially due to the slow deactivation of ChR2 channels. Tkatch *et al.* (25) showed that optogenetic-induced mitochondrial depolarization can recover slowly in cells expressing the ChR(SSFO) mutant. Alternatively, co-expressing Channelrhodopsin and Bacteriorhodopsin or Archaerhodopsins in the IMM and stimulating cells with alternating blue and yellow light might achieve reversible control of $\Delta\Psi_m$. The energetic states or types of cell may also affect the feasibility of inducing faster or more reversible mitochondrial depolarization. For instance, mitochondrial oscillations can be readily triggered in isolated guinea pig cardiomyocytes (7,9), but it is much more difficult in isolated mouse cardiomyocytes.

In summary, we have developed and characterized a mitochondrial optogenetics approach to induce targeted mitochondrial depolarization, which provides an alternative to the traditional optical or pharmacological means of modulating MMP and $\Delta\Psi_m$ to understand their roles in determining cell fate. We expect the research tools shown here and the knowledge acquired will facilitate the design of novel optogenetic-based therapeutic strategies for the treatment of diseases involving mitochondrial dysfunction.

Experimental procedures

Cell culture. HeLa and H9C2 cells were obtained from ATCC and cultured in Dulbecco's Modified Eagle Medium (Gibco) supplemented with 10% (v/v) Fetal Bovine Serum (Gibco) and 2 mM L-Glutamine (Gibco). Cells were maintained in 5% CO_2 at 37 °C with confluence between 10% and 80%. hiPSC-CMs were reprogrammed from human cardiac fibroblasts as described previously (55) and maintained on Matrigel Membrane Matrix (Thermo Fisher Scientific) in mTeSR™ medium (Stem Cell Technologies) until 75% confluency. CM differentiation was performed by using a small molecule–based protocol as described previously (56,57). Beating hiPSC-CM began to appear 9-12 days after differentiation was initiated.

Plasmid construction. The ROMK and ABCB10(1-140bp) (named ABCB for simplification) MLS were synthesized by GeneArt (Life Technologies). pCMV-myc-mito vector was purchased from Life Technologies (catalog number V82220), and pLenti-EF1a-hChR2(H134R)-EYFP-WPRE was a gift from Karl Deisseroth (Addgene plasmid # 20942). To construct the CMV-myc-mito based plasmids (e.g. pCMV-mito-ChR2-eYFP), pCMV-myc-mito-GFP vector was digested with SalI and XbaI and ligated with ChR2-eYFP fragment obtained from pLenti-EF1a-hChR2(H134R)-EYFP-WPRE vector *via* PCR. The ROMK based plasmid was constructed by replacing the mito sequence with the ROMMK sequence. The pCAG-ABCB-ChR2-eYFP and pCAG-ABCB-eYFP vectors were constructed using the Gibson Ligation Kit following the manufacturer's instructions. The sequences of constructed vectors were confirmed by DNA sequencing at the University of Alabama at Birmingham Helfin Center Genetics Core.

Adenovirus production. The gene of interest (i.e. CMV-ABCB140-ChR2-YFP-ER) was PCR amplified from vector pCAG-CMV-ABCB-ChR2-eYFP using blunt-end primers. This gene fragment was cloned into the pENTR-D-TOPO vector purchased from Life Technologies (catalog number K2400) to generate the adenovirus entry vector. The entry vector sequence was confirmed using the M13 Forward and M13 Reverse primers. Adenoviral expression vector was constructed by LR recombination using the ViraPower™ Adenoviral Gateway™ Expression Kit (Life technologies catalog number K4930). To produce adenovirus, the expression vector was digested with PacI, purified, and then transfected into HEK 293A cells pre-seeded in T-flasks using Lipofectamine 2000. Cells were cultured until visible regions of cytopathic effect were observed in approximately 80% of the culture. Cells were then squirted from the flask bottom and lysed via three successive freeze/thaw cycles to release the crude adenovirus. To amplify the adenovirus, 293A cells were infected with the crude adenovirus at a MOI of approximately 5. High titer adenovirus was harvested as described above when the 293A cells were floating or lightly attached to the culture dish, 2-3 days after infection.

Confocal imaging and colocalization analysis. Vectors containing ChR2-eFYP or eYFP with various MLS (e.g., mito, ROMK and ABCB) were transfected to H9C2 or HeLa cells cultured on a 15mm glass-bottom dish using the Lipofectoamine 3000 transfection reagent. hiPSC-CMs were transduced with the adenovirus containing ABCB-ChR2-eYFP at MOI of 50. 48 hours after transfection/transduction, cells were loaded with MitoTracker Deep Red (250 nM) for 30 minutes. The 515nm argon laser and 635nm LD laser lines of an Olympus FV1000 confocal microscope

were used to image eYFP and MitoTracker, respectively. Images were processed offline using ImageJ software (Wayne Rasband, NIH) for colocalization analysis.

Light illumination-induced targeted mitochondrial depolarization. The ABCB-ChR2-eYFP or ABCB-eYFP-expressing H9C2 cells were loaded with mitochondrial membrane potential fluorescent dye TMRM (20 nM) and illuminated with 475nm LED pulses (5 mW/mm^2). The blue light was delivered by a 10X objective lens coupled to a LED driver, which was controlled by a Myopacer stimulator (IonOptix, Westwood, MA). The fluorescence of TMRM during light illumination was recorded using an Olympus FV1000 confocal microscope and analyzed using ImageJ software.

Cell death and cytotoxicity assay. ABCB-ChR2-eYFP-expressing or control (i.e., ABCB-eYFP expressing, mock transfected and un-transfected) cells were illuminated by LED light of different duration and irradiance (as indicated in the figure legends). Right after light treatment cells were detached with 0.25% Trypsin-EDTA, stained with Trypan Blue, and counted using a hemocytometer as described previously (24). The cytotoxicity and cell viability were also measured using the LDH assay and AlamarBlue (AB) assay, respectively. For the LDH assay, at the end of light illumination, 200 μl cell culture medium was removed and added to a 96 well plate, 100 μl of the reaction mixture was added to each well and the plate was incubated for 30 minutes at room temperature, protected from light. The absorbance was measured at 490nm and 680nm using a microplate reader. LDH activity was calculated following the manufacture's instruction. For the AB assay, 10 μl AlamarBlue reagent was directly added to cells in 100 μl culture medium. Cell cultures were incubated for 4 hours in an incubator (37 °C, protected from light). The absorbance was measured at 570nm using a spectrometer.

Immunocytochemistry. Cells cultured on 15 mm coverslips were fixed in 4% Formaldehyde in PBS and then treated with PBS containing 10% goat serum and 0.3% Triton® X-100 to block non-specific staining. Cells were stained with the following primary antibodies: ChR2, TOMM20, LC3, ATP5A, or Cytochrome C at a ratio of 1:200. After overnight room temperature incubation, secondary antibodies AlexaFluor 555 and/or AlexaFluor 647 were diluted in 1% BSA, 1% goat serum, 0.3% Triton® X-100 in PBS at a ratio of 1:200, and then added to the cells. Coverslips were mounted on slides and imaged using an Olympus FV1000 confocal microscope.

Parkin translocation assay. HeLa cells were co-transfected with plasmid DNA encoding mCherry-tagged Parkin (37) (Addgene plasmid #23956;) and DNA encoding either ABCB-ChR2-YFP or ABCB-YFP using the Neon Transfection System (Invitrogen) and seeded in 35 mm glass-bottom dishes (MatTek, Ashland, MA). Two days after transfection cells were subjected to LED illumination (0.5 mW/mm^2, 24 hours). Confocal imaging of YFP and mCherry expression and localization was done immediately before treatment, and after 4, 8, and 24 hours of treatment, using an Olympus FV1000 confocal microscope.

Flow Cytometry. Cells were trypsinized, centrifuged down, and washed twice with PBS before resuspension in staining buffer (10 mM HEPES/NaOH (pH 7.4), 140 mM NaCl, 2.5 mM $CaCl_2$) containing working concentrations of Mitoview 633 (25 nM) and stained following the manufacture's instruction. Cells were then centrifuged down and washed twice with PBS + 1% BSA before analysis with a BD LSR II Flow Cytometer (BD Biosciences, San Jose, CA).

Materials. Mouse monoclonal antibodies for GFP, ATP5A, TOM20 and LC3 were purchased from Abcam (Cambridge, MA). Mouse monoclonal ChR2 antibody was obtained from Progen (Heidelberg, Germany). Oregon Green 488 anti-rabbit IgG, MitoSox, TMRM, and MitoTracker Deep Red FM were purchased from Life Technologies (Carlsbad, CA). MitoView 633 was purchased from Biotium (Fremont, CA). All other reagents were from Sigma (St Louis, MO).

Statistics. Analysis and presentation of the data were performed using OriginLab software (Northampton, MA). Comparisons between groups were performed using paired or unpaired 2-tailed Student's t test. Data were considered significantly different at $p < 0.05$ or below. Results are presented as mean $\pm$ SEM.

Materials & Correspondence. All relevant materials that support our experimental findings are available from the corresponding author upon reasonable request.

Acknowledgements

The authors acknowledge K. Goh and Q. Li for their technical support. This work is supported by National Institute of Health (NIH) R21 HL127599 and R01 HL121206 (to L.Z.)

Competing interests

The authors declare no competing interests.

References

1. Honda, H. M., Korge, P., and Weiss, J. N. (2005) Mitochondria and ischemia/reperfusion injury. *Annals of the New York Academy of Sciences* **1047**, 248-258
2. Wallace, D. C., and Fan, W. (2009) The pathophysiology of mitochondrial disease as modeled in the mouse. *Genes & development* **23**, 1714-1736
3. Desagher, S., and Martinou, J. C. (2000) Mitochondria as the central control point of apoptosis. *Trends Cell Biol* **10**, 369-377
4. Weisova, P., Anilkumar, U., Ryan, C., Concannon, C. G., Prehn, J. H., and Ward, M. W. (2012) 'Mild mitochondrial uncoupling' induced protection against neuronal excitotoxicity requires AMPK activity. *Biochimica et biophysica acta* **1817**, 744-753
5. Brennan, J. P., Southworth, R., Medina, R. A., Davidson, S. M., Duchen, M. R., and Shattock, M. J. (2006) Mitochondrial uncoupling, with low concentration FCCP, induces ROS-dependent cardioprotection independent of KATP channel activation. *Cardiovascular research* **72**, 313-321
6. Hausenloy, D. J., Maddock, H. L., Baxter, G. F., and Yellon, D. M. (2002) Inhibiting mitochondrial permeability transition pore opening: a new paradigm for myocardial preconditioning? *Cardiovascular research* **55**, 534-543
7. Aon, M. A., Cortassa, S., Marban, E., and O'Rourke, B. (2003) Synchronized whole cell oscillations in mitochondrial metabolism triggered by a local release of reactive oxygen species in cardiac myocytes. *The Journal of biological chemistry* **278**, 44735-44744
8. Brady, N. R., Elmore, S. P., van Beek, J. J., Krab, K., Courtoy, P. J., Hue, L., and Westerhoff, H. V. (2004) Coordinated behavior of mitochondria in both space and time: a reactive oxygen species-activated wave of mitochondrial depolarization. *Biophysical journal* **87**, 2022-2034
9. Zhou, L., Aon, M. A., Liu, T., and O'Rourke, B. (2011) Dynamic modulation of Ca(2+) sparks by mitochondrial oscillations in isolated guinea pig cardiomyocytes under oxidative stress. *Journal of molecular and cellular cardiology* **51**, 632-639
10. Boyden, E. S. (2011) A history of optogenetics: the development of tools for controlling brain circuits with light. *F1000 biology reports* **3**, 11
11. Boyden, E. S., Zhang, F., Bamberg, E., Nagel, G., and Deisseroth, K. (2005) Millisecond-timescale, genetically targeted optical control of neural activity. *Nature neuroscience* **8**, 1263-1268
12. Deisseroth, K. (2011) Optogenetics. *Nature methods* **8**, 26-29
13. Zhang, F., Wang, L. P., Boyden, E. S., and Deisseroth, K. (2006) Channelrhodopsin-2 and optical control of excitable cells. *Nature methods* **3**, 785-792
14. Adams, D. S., Tseng, A. S., and Levin, M. (2013) Light-activation of the Archaerhodopsin H(+)-pump reverses age-dependent loss of vertebrate regeneration: sparking system-level controls in vivo. *Biology open* **2**, 306-313
15. Gradinaru, V., Thompson, K. R., and Deisseroth, K. (2008) eNpHR: a Natronomonas halorhodopsin enhanced for optogenetic applications. *Brain cell biology* **36**, 129-139
16. Nagel, G., Szellas, T., Huhn, W., Kateriya, S., Adeishvili, N., Berthold, P., Ollig, D., Hegemann, P., and Bamberg, E. (2003) Channelrhodopsin-2, a directly light-gated cation-selective membrane channel. *Proceedings of the National Academy of Sciences of the United States of America* **100**, 13940-13945
17. Hegemann, P., Gartner, W., and Uhl, R. (1991) All-trans retinal constitutes the functional chromophore in Chlamydomonas rhodopsin. *Biophysical journal* **60**, 1477-1489
18. Rein, M. L., and Deussing, J. M. (2012) The optogenetic (r)evolution. *Molecular genetics and genomics : MGG* **287**, 95-109
19. Arrenberg, A. B., Stainier, D. Y., Baier, H., and Huisken, J. (2010) Optogenetic control of cardiac function. *Science* **330**, 971-974

20. Bruegmann, T., Malan, D., Hesse, M., Beiert, T., Fuegemann, C. J., Fleischmann, B. K., and Sasse, P. (2010) Optogenetic control of heart muscle in vitro and in vivo. *Nature methods* **7**, 897-900
21. Entcheva, E. (2013) Cardiac Optogenetics. *American journal of physiology. Heart and circulatory physiology*
22. Asano, T., Ishizua, T., and Yawo, H. (2012) Optically controlled contraction of photosensitive skeletal muscle cells. *Biotechnology and bioengineering* **109**, 199-204
23. Jia, Z., Valiunas, V., Lu, Z., Bien, H., Liu, H., Wang, H. Z., Rosati, B., Brink, P. R., Cohen, I. S., and Entcheva, E. (2011) Stimulating cardiac muscle by light: cardiac optogenetics by cell delivery. *Circulation. Arrhythmia and electrophysiology* **4**, 753-760
24. Li, Q., Ni, R. R., Hong, H., Goh, K. Y., Rossi, M., Fast, V. G., and Zhou, L. (2017) Electrophysiological Properties and Viability of Neonatal Rat Ventricular Myocyte Cultures with Inducible ChR2 Expression. *Sci Rep* **7**, 1531
25. Tkatch, T., Greotti, E., Baranauskas, G., Pendin, D., Roy, S., Nita, L. I., Wettmarshausen, J., Prigge, M., Yizhar, O., Shirihai, O. S., Fishman, D., Hershfinkel, M., Fleidervish, I. A., Perocchi, F., Pozzan, T., and Sekler, I. (2017) Optogenetic control of mitochondrial metabolism and Ca2+ signaling by mitochondria-targeted opsins. *Proceedings of the National Academy of Sciences* **114**, E5167-E5176
26. Ernst, P., Xu, N., Goh, K., O'Rourke, B., Zhang, J. J., Liu, M. X., and Zhou, L. (2017) Abstract 24059: Optogenetic-induced Mitochondrial Membrane Potential Depolarization and Targeting Cell Death. *Circulation* **136**, A24059-A24059
27. Yang, F., Tu, J., Pan, J. Q., Luo, H. L., Liu, Y. H., Wan, J., Zhang, J., Wei, P. F., Jiang, T., Chen, Y. H., and Wang, L. P. (2013) Light-controlled inhibition of malignant glioma by opsin gene transfer. *Cell death & disease* **4**, e893
28. Hill, R. A., Damisah, E. C., Chen, F., Kwan, A. C., and Grutzendler, J. (2017) Targeted two-photon chemical apoptotic ablation of defined cell types in vivo. *Nat Commun* **8**, 15837
29. Karbowski, M., Arnoult, D., Chen, H., Chan, D. C., Smith, C. L., and Youle, R. J. (2004) Quantitation of mitochondrial dynamics by photolabeling of individual organelles shows that mitochondrial fusion is blocked during the Bax activation phase of apoptosis. *The Journal of cell biology* **164**, 493-499
30. Kettlewell, S., Cabrero, P., Nicklin, S. A., Dow, J. A., Davies, S., and Smith, G. L. (2009) Changes of intra-mitochondrial Ca2+ in adult ventricular cardiomyocytes examined using a novel fluorescent Ca2+ indicator targeted to mitochondria. *J Mol Cell Cardiol* **46**, 891-901
31. Nagel, G., Brauner, M., Liewald, J. F., Adeishvili, N., Bamberg, E., and Gottschalk, A. (2005) Light activation of channelrhodopsin-2 in excitable cells of Caenorhabditis elegans triggers rapid behavioral responses. *Current biology : CB* **15**, 2279-2284
32. Foster, D. B., Ho, A. S., Rucker, J., Garlid, A. O., Chen, L., Sidor, A., Garlid, K. D., and O'Rourke, B. (2012) Mitochondrial ROMK channel is a molecular component of mitoK(ATP). *Circulation research* **111**, 446-454
33. Higgins, C. F. (1992) ABC transporters: from microorganisms to man. *Annual review of cell biology* **8**, 67-113
34. Higgins, C. F. (2001) ABC transporters: physiology, structure and mechanism--an overview. *Research in microbiology* **152**, 205-210
35. Graf, S. A., Haigh, S. E., Corson, E. D., and Shirihai, O. S. (2004) Targeting, import, and dimerization of a mammalian mitochondrial ATP binding cassette (ABC) transporter, ABCB10 (ABC-me). *The Journal of biological chemistry* **279**, 42954-42963
36. Miyazaki, E., Kida, Y., Mihara, K., and Sakaguchi, M. (2005) Switching the sorting mode of membrane proteins from cotranslational endoplasmic reticulum targeting to posttranslational mitochondrial import. *Molecular biology of the cell* **16**, 1788-1799

37. Narendra, D., Tanaka, A., Suen, D. F., and Youle, R. J. (2008) Parkin is recruited selectively to impaired mitochondria and promotes their autophagy. *The Journal of cell biology* **183**, 795-803
38. Carroll, R. G., Hollville, E., and Martin, S. J. (2014) Parkin sensitizes toward apoptosis induced by mitochondrial depolarization through promoting degradation of Mcl-1. *Cell Rep* **9**, 1538-1553
39. Zhang, C., Lee, S., Peng, Y., Bunker, E., Giaime, E., Shen, J., Zhou, Z., and Liu, X. (2014) PINK1 triggers autocatalytic activation of Parkin to specify cell fate decisions. *Current biology : CB* **24**, 1854-1865
40. Ashrafi, G., Schlehe, J. S., LaVoie, M. J., and Schwarz, T. L. (2014) Mitophagy of damaged mitochondria occurs locally in distal neuronal axons and requires PINK1 and Parkin. *The Journal of cell biology* **206**, 655-670
41. Cai, Q., Zakaria, H. M., Simone, A., and Sheng, Z. H. (2012) Spatial parkin translocation and degradation of damaged mitochondria via mitophagy in live cortical neurons. *Current biology : CB* **22**, 545-552
42. Burke, R. E., and O'Malley, K. (2013) Axon degeneration in Parkinson's disease. *Exp Neurol* **246**, 72-83
43. Hollenbeck, P. J., Bray, D., and Adams, R. J. (1985) Effects of the uncoupling agents FCCP and CCCP on the saltatory movements of cytoplasmic organelles. *Cell Biol Int Rep* **9**, 193-199
44. Berezhnov, A. V., Soutar, M. P., Fedotova, E. I., Frolova, M. S., Plun-Favreau, H., Zinchenko, V. P., and Abramov, A. Y. (2016) Intracellular pH Modulates Autophagy and Mitophagy. *The Journal of biological chemistry* **291**, 8701-8708
45. Doebler, J. A. (2000) Effects of protonophores on membrane electrical characteristics in NG108-15 cells. *Neurochem Res* **25**, 263-268
46. To, M. S., Aromataris, E. C., Castro, J., Roberts, M. L., Barritt, G. J., and Rychkov, G. Y. (2010) Mitochondrial uncoupler FCCP activates proton conductance but does not block store-operated Ca(2+) current in liver cells. *Arch Biochem Biophys* **495**, 152-158
47. Baines, C. P., Kaiser, R. A., Sheiko, T., Craigen, W. J., and Molkentin, J. D. (2007) Voltage-dependent anion channels are dispensable for mitochondrial-dependent cell death. *Nat Cell Biol* **9**, 550-555
48. Kim, C. N., Wang, X., Huang, Y., Ibrado, A. M., Liu, L., Fang, G., and Bhalla, K. (1997) Overexpression of Bcl-X(L) inhibits Ara-C-induced mitochondrial loss of cytochrome c and other perturbations that activate the molecular cascade of apoptosis. *Cancer Res* **57**, 3115-3120
49. Wang, C., and Youle, R. J. (2009) The role of mitochondria in apoptosis*. *Annu Rev Genet* **43**, 95-118
50. Kitada, T., Asakawa, S., Hattori, N., Matsumine, H., Yamamura, Y., Minoshima, S., Yokochi, M., Mizuno, Y., and Shimizu, N. (1998) Mutations in the parkin gene cause autosomal recessive juvenile parkinsonism. *Nature* **392**, 605-608
51. Dai, H., Deng, Y., Zhang, J., Han, H., Zhao, M., Li, Y., Zhang, C., Tian, J., Bing, G., and Zhao, L. (2015) PINK1/Parkin-mediated mitophagy alleviates chlorpyrifos-induced apoptosis in SH-SY5Y cells. *Toxicology* **334**, 72-80
52. Zhao, C., Chen, Z., Xu, X., An, X., Duan, S., Huang, Z., Zhang, C., Wu, L., Zhang, B., Zhang, A., Xing, C., and Yuan, Y. (2017) Pink1/Parkin-mediated mitophagy play a protective role in cisplatin induced renal tubular epithelial cells injury. *Exp Cell Res* **350**, 390-397
53. Zhang, H. T., Mi, L., Wang, T., Yuan, L., Li, X. H., Dong, L. S., Zhao, P., Fu, J. L., Yao, B. Y., and Zhou, Z. C. (2016) PINK1/Parkin-mediated mitophagy play a protective role in manganese induced apoptosis in SH-SY5Y cells. *Toxicol In Vitro* **34**, 212-219
54. Yizhar, O., Fenno, L. E., Prigge, M., Schneider, F., Davidson, T. J., O'Shea, D. J., Sohal, V. S., Goshen, I., Finkelstein, J., Paz, J. T., Stehfest, K., Fudim, R., Ramakrishnan, C.,

Huguenard, J. R., Hegemann, P., and Deisseroth, K. (2011) Neocortical excitation/inhibition balance in information processing and social dysfunction. *Nature* **477**, 171-178

55. Zhang, L., Guo, J., Zhang, P., Xiong, Q., Wu, S. C., Xia, L., Roy, S. S., Tolar, J., O'Connell, T. D., Kyba, M., Liao, K., and Zhang, J. (2015) Derivation and high engraftment of patient-specific cardiomyocyte sheet using induced pluripotent stem cells generated from adult cardiac fibroblast. *Circ Heart Fail* **8**, 156-166
56. Zhu, W., Gao, L., and Zhang, J. (2017) Pluripotent Stem Cell Derived Cardiac Cells for Myocardial Repair. *J Vis Exp*
57. Gao, L., Kupfer, M. E., Jung, J. P., Yang, L., Zhang, P., Da Sie, Y., Tran, Q., Ajeti, V., Freeman, B. T., Fast, V. G., Campagnola, P. J., Ogle, B. M., and Zhang, J. (2017) Myocardial Tissue Engineering With Cells Derived From Human-Induced Pluripotent Stem Cells and a Native-Like, High-Resolution, 3-Dimensionally Printed Scaffold. *Circ Res* **120**, 1318-1325

Figure Legends

Figure 1. Representative confocal images showing cellular localization of ChR2-eYFP or eYFP in different types of cells. A: H9C2 cells expressing ABCB-eYFP; B: H2C2 cells expressing ABCB-ChR2-eYFP; C: Immunoblotting of H9C2 cells expressing ABCB-ChR2-eFYP with ChR2 antibody; D HeLa cells expressing ABCB-ChR2-eYFP; and (E) hiPSC-CMs expressing ABCB-ChR2-eYFP. In all experiments cells were stained with MitoTracker Deep Red (250 nM). Yellow color indicates colocalization of ChR2-eYFP (or eYFP) and the mitochondrial marker.

Figure 2. Light-elicited targeted mitochondrial depolarization in H9C2 cells expressing ABCB-ChR2-eYFP. A: Schematic figure showing that cells in zone 1 were receiving illumination by LED pulses (5 mW/mm^2) and cells in zone 2 were not exposed to illumination. B and C: Confocal images showing mitochondrial membrane potential, measured by TMRM fluorescent dye (20 nM), in cells before (B) and after (C) light illumination. D: Averaged mitochondrial membrane potential of cells in zone 1 and zone 2 before and after light illumination. A total of four cell cultures were examined.

Figure 3. Light illumination induces Parkin mitochondrial translocation in ABCB-ChR2-eYFP-expressing HeLa cells but not in ABCB-eYFP-expressing HeLa cells. A-C: Representative confocal imagines showing localization of Parkin-mCherry in light illuminated cells expressing ABCB-ChR2-eYFP and Parkin-mCherry (A), light illuminated cells expressing ABCB- eYFP and Parkin-mCherry (B), and non-illuminated cells expressing ABCB-ChR2-eYFP and Parkin-mCherry (C). Images were taken at 0, 4, 8, and 24 hours during light illumination. Red represents Parkin-mCherry, green represents eYFP, and merge represents Parkin accumulation in mitochondria.

Figure 4. Light illumination induces targeted cell death in HeLa cells expressing ABCB-ChR2-eYFP. A: Representative transmitted light images of ABCB-ChR2-eYFP or ABCB-eYFP-expressing cells with or without illumination by LED pulses (0.5 mW/mm^2, 24 hours). B and C: Comparison of cell viability measured by LDH assay (B) and cytotoxicity measured by alamarBlue assay (C) in ABCB-ChR2-eYFP or ABCB-eYFP cells with or without the presence of LED illumination. D and E: Effect of the mPTP blocker, CsA, on cell viability (D) and cytotoxicity (E) in ABCB-ChR2-eYFP-expressing or control cell cultures with or without LED illumination. N represents the number of cell cultures.

Figure 5. Time and light irradiance dependence of mitochondrial optogenetic-mediated cell death. A: Time dependence of LED illumination (0.5 mW/mm^2)-induced cell death in ABCB-ChR2-eYFP-expressing HeLa cultures. Four cell cultures were repeated at each time point. Cell viability was determined using the trypan blue cell counting method. B: LED irradiance dependence of illumination-elicited cell death. ABCB-ChR2-eYFP or control (mock-transfected) HeLa cultures were illuminated by LED of various intensity for six hours. At least four cell cultures were repeated for a group. Cell death were measured by PI/DAPI staining. C: Representative images of PI staining in cultures illuminated by LED of different irradiance.

Figure 6. Mitochondrial optogenetics induces cell death *via* apoptotic pathways. A: Z-VAD-FMK, a general caspase inhibitor, substantially reduced light-elicited cell death in HeLa cell cultures expressing ABCB-ChR2. 7-Cl-O-Nec-1, a necroptosis inhibitor, had no significant effect on the light-induced cell death. n represents the numbers of cell cultures. B: Z-VAD-FMK alleviated light-induced mitochondrial depolarization in ABCB-ChR2 expressing cells. C: Light illumination induced cytochrome C release into cytosol in ABCB-ChR2-expressing cells.

Figure 7. Effects of Parkin activation on mitochondrial optogenetic-mediated cell death. A: Flow cytometry showing that Parkin activation exacerbated light-induced mitochondrial depolarization in 24 hours. B: Parkin activation did not influence viability of HeLa cells within 24 hours light illumination but promoted cell death 24 hours later after stopping light illumination. n represents the number of cell cultures.

Figure 8. Mild, short-term light illumination protects ABCB-ChR2-expressing cells against apoptotic cell death. Representative images of Hoechst and Propidium Iodide (PI) staining in cultures illuminated by LED of moderate irradiance (4 mW/mm^2 for 6 hours) without (A) or with (B) light-induced (0.2 mW/mm^2 for 2 hours) mitochondrial preconditioning. C: Summary of cell viability in the control (i.e. without light pretreatment) and preconditioned (i.e. with light pretreatment) groups. n=3 for each group.

Figure 1

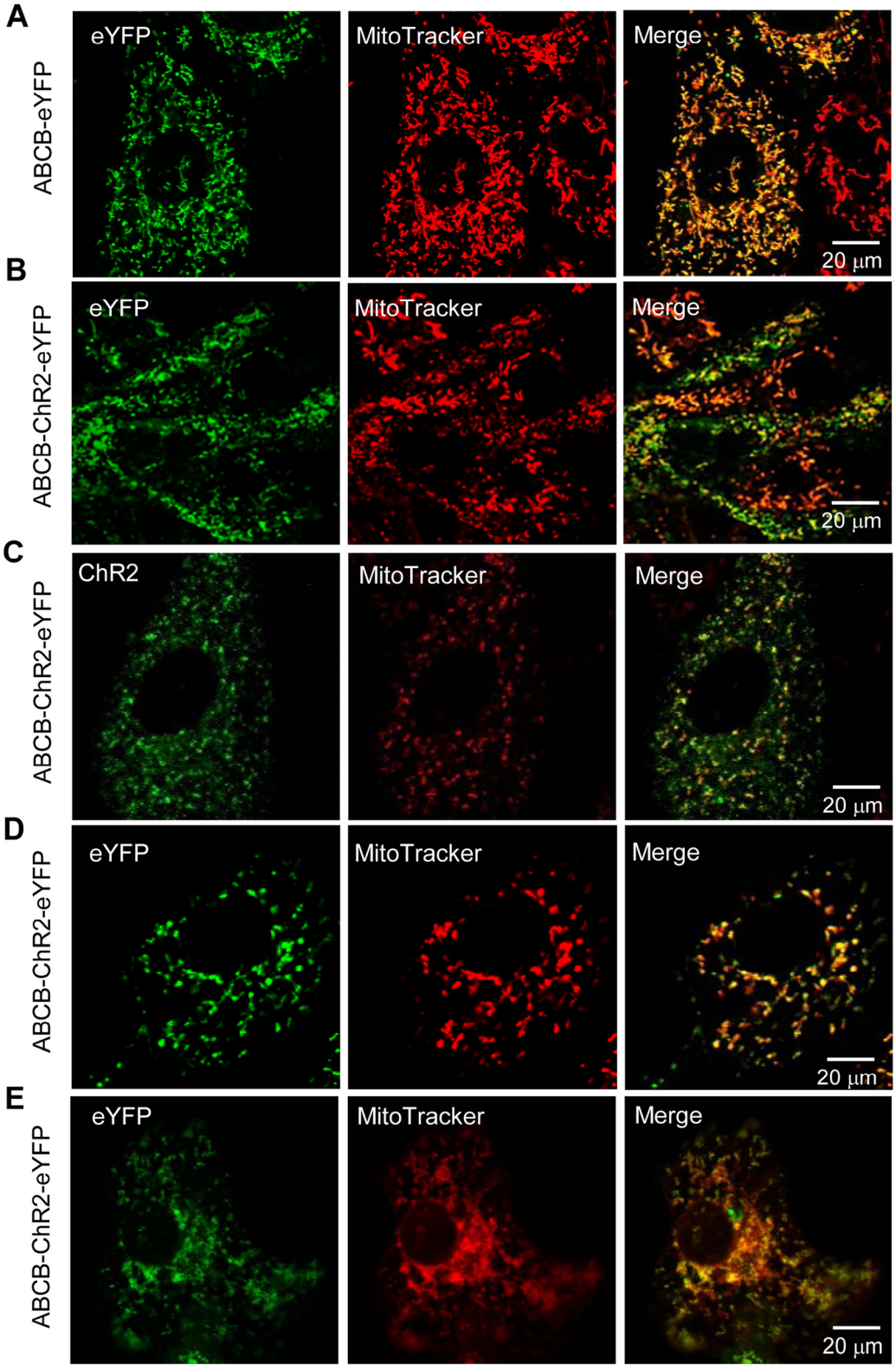

Figure 2

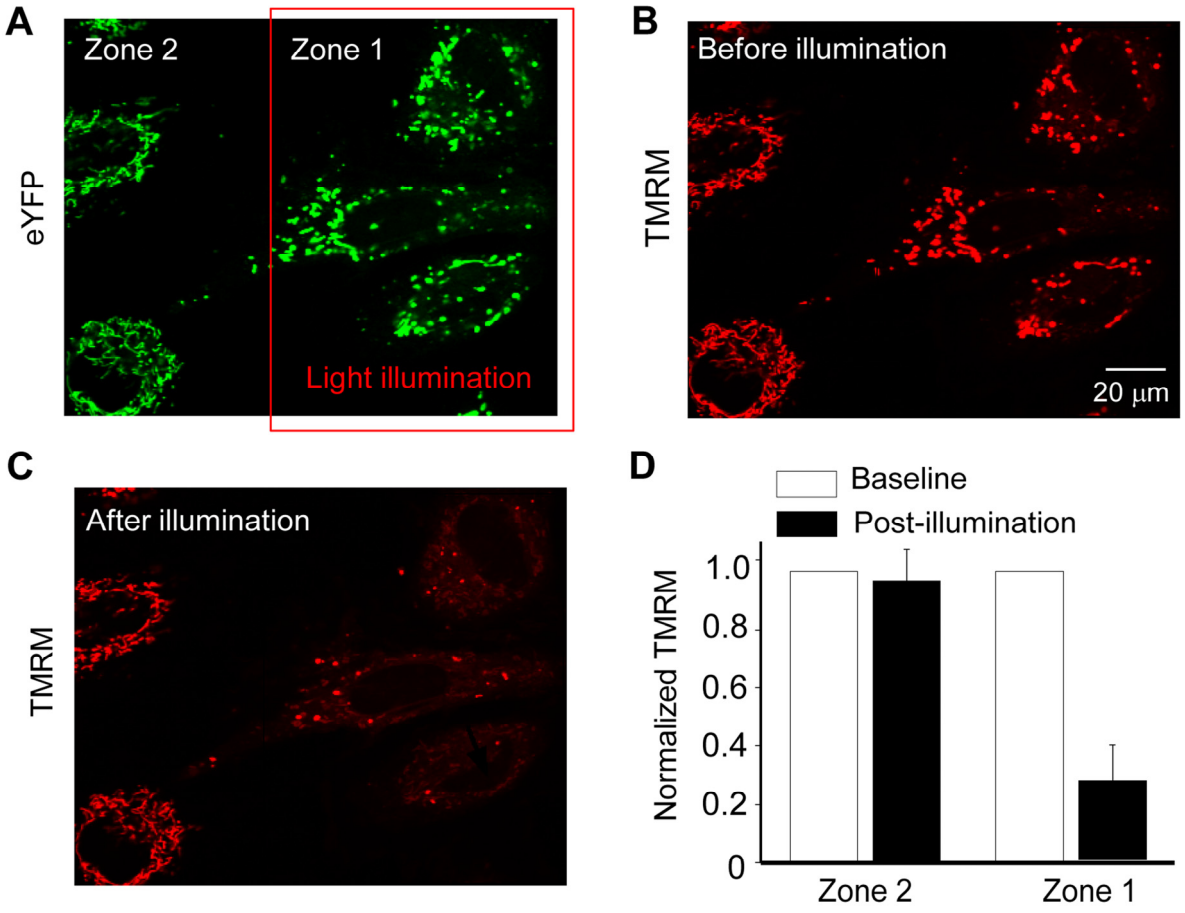

Figure 3

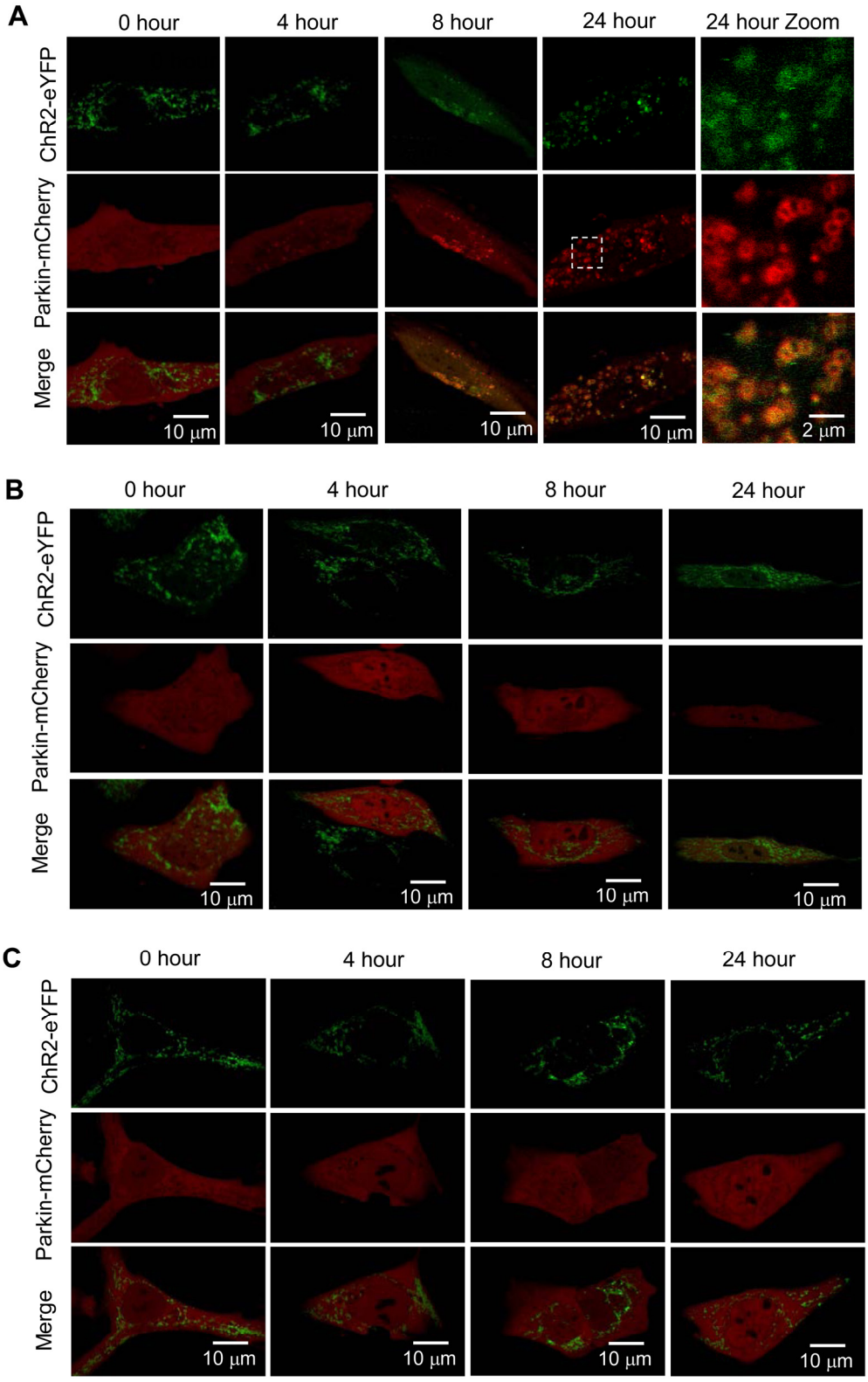

Figure 4

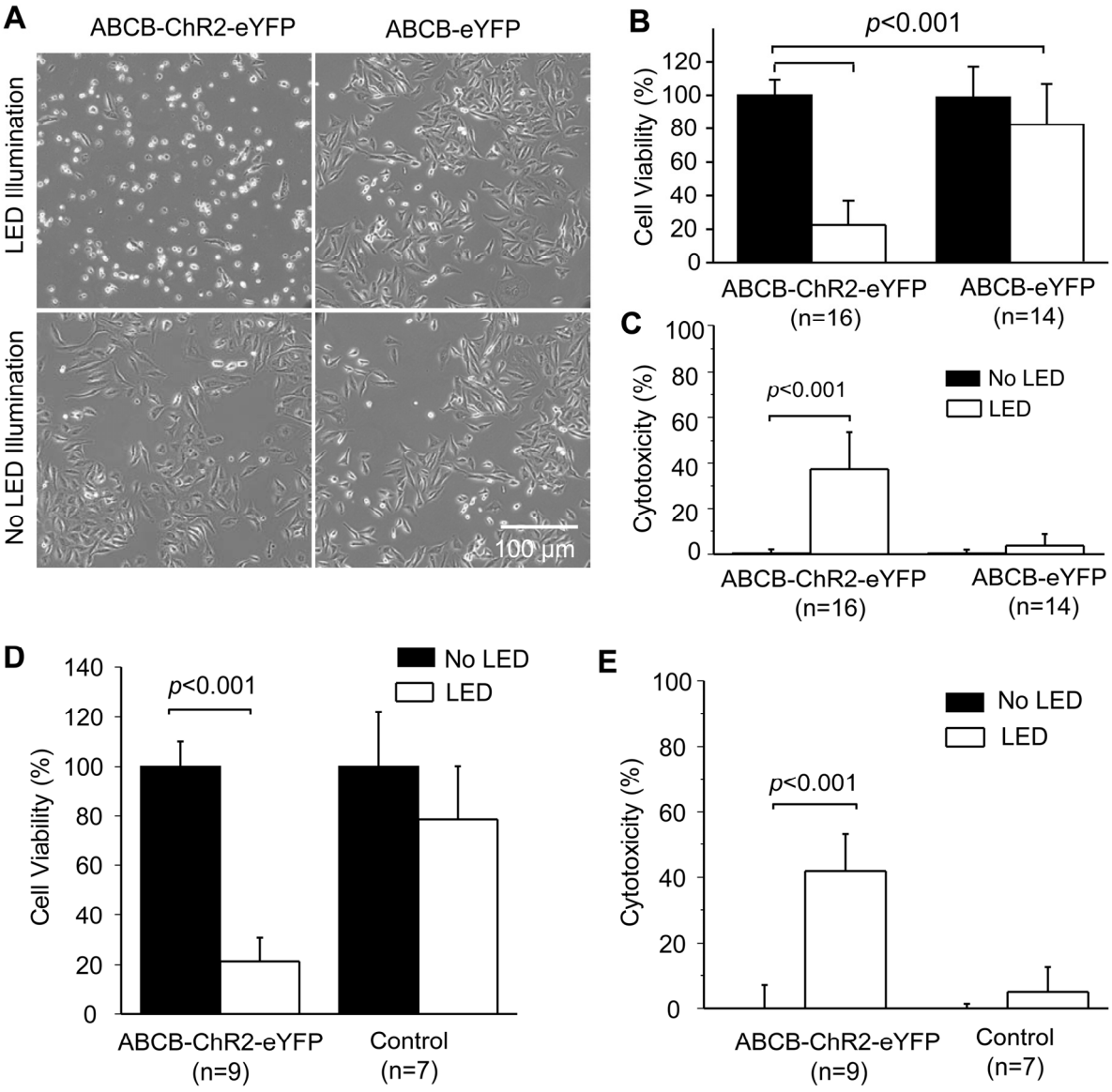

Figure 5

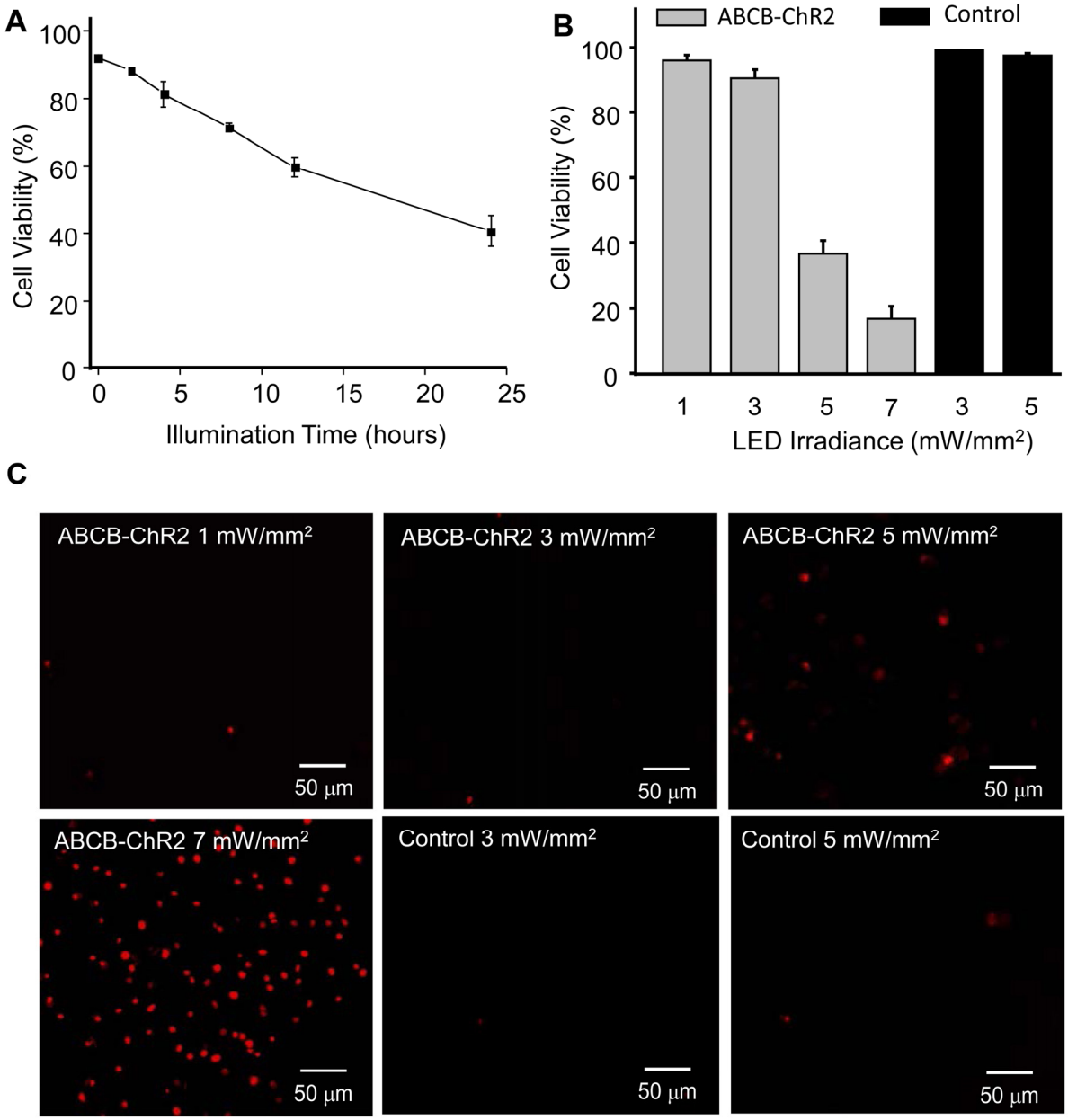

Figure 6

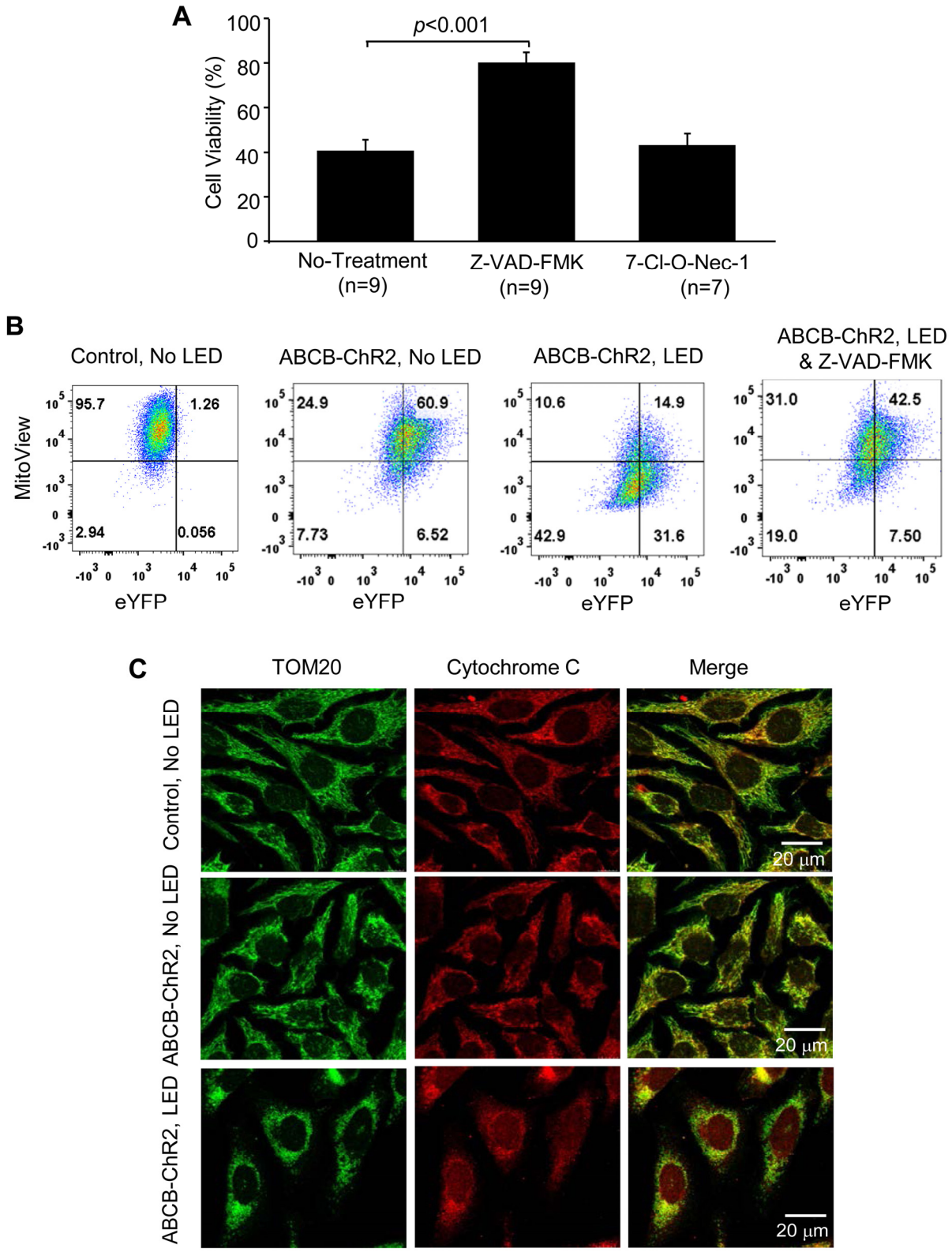

Figure 7

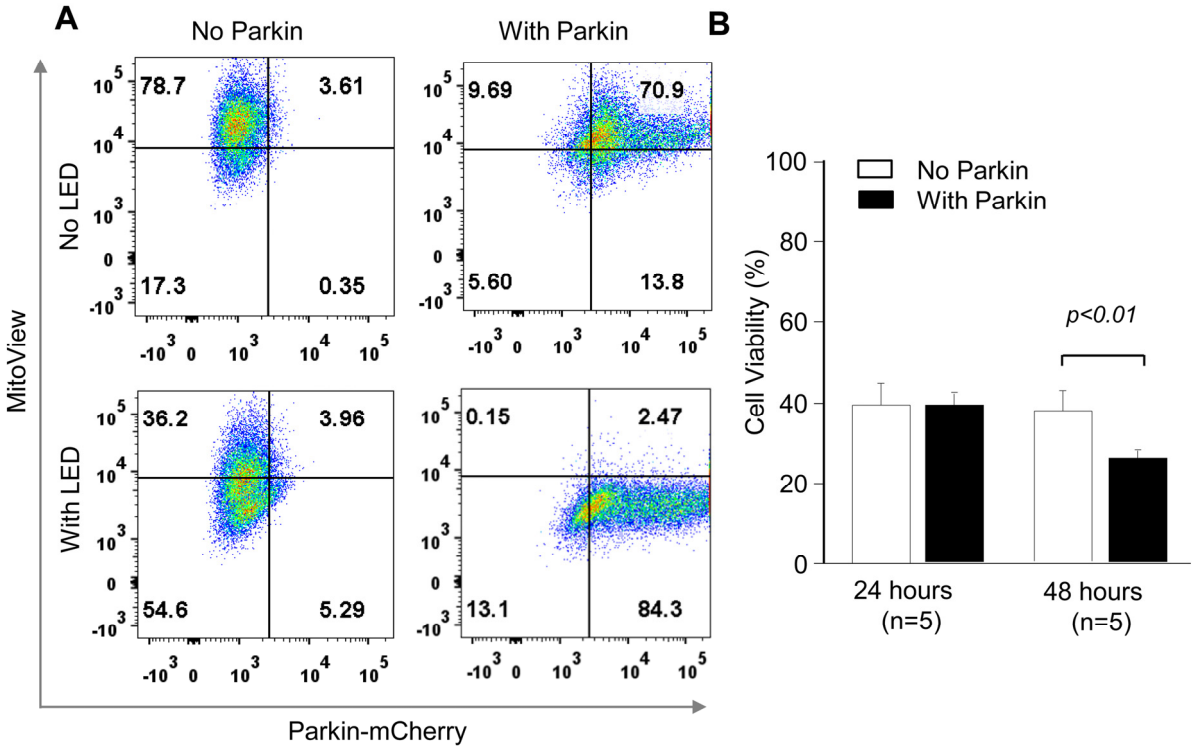

Figure 8